7 Particle Size Distribution and Monodisperse Sols

Monodisperse systems are those containing particles of almost the same size within a deviation of about 10 percent. The chemical structure, shape, etc. are in general the same and the system may be treated as a standard or basic disperse system for understanding general disperse systems. However, the systems that usually appear are polydisperse, having various particle sizes.

7.1 Particle Size Distribution

In Chapt. 6, experimental methods are described to determine a particle size. But, if the solution is polydisperse, some of the methods provide only a kind of average representing the particle size. For example, the turbidity of Eq. 6.4 is related to the weight-averaged molecular weight of the system under observation, or the square of the particle mass averaged over the size distribution. Conversely, these data can hardly be analyzed for the size distribution function unless a well prepared set of monodisperse systems is used. This is true with sedimentation.

As noted in Sec. 6.2.1.1, if the Debye factor has to be introduced in Eq. 6.1, the anguleular intensity distribution of scattered light from noninteracting particles is influenced by the size, shape, and optical contrast of the particles. We may assume that the shape of the particles is known, as given by the Debye factor listed in Table 6.1. The size distribution function, $G(M)$, where M is the particle mass, can appear in the expression of the scattered intensity as given by

$$\frac{I_\theta(q)}{I_{\mathrm{i,u}}} = \frac{\pi^2(1+\cos^2\theta)}{2\varepsilon_0^2\lambda^4 R^2}\alpha_0^2 \int_0^\infty G(M)M^2P(q,M)\mathrm{d}M \tag{7.1}$$

where α_0 is the particle polarizability per unit mass so that $\alpha = \alpha_0 M$. By inversion of the Fredholm equation, Eq. 7.1, $G(M)$ can be experimentally determined from the measurement of the scattered intensity as a function of the scattering angle. Schnablegger and Glatter (1993) describe the computational procedures.

On the other hand, observations using microscopes give individual particle sizes and lead to determination of the distribution. It may also be obtained by observing speckles in an ultramicroscope, since the speckle intensity is related to the particle size (volume). The Coulter counter may be used for an individual size determination by means of pulse height.

When dynamic light scattering is used for a polydisperse system of spherical particles, the particles are divided into groups depending on their sizes. If there is no interaction among particles, the first-order photon correlation function, $g^{(1)}(\tau)$, is given by the weighted sum of the type of exp $(-\Gamma_j\tau)$, Eq. 6.22, for group j:

$$g^{(1)}(\tau) = \sum_j g_j \exp(-\Gamma_j\tau) / \sum_j g_j \equiv \exp(-\Gamma\tau) \tag{7.2}$$

where Γ_j is the decay rate for the particle belonging to the j-th group and $g_j = |\alpha_j|^2 N_j$, α_j and N_j being the particle polarizability and the number of particles in the j-th group, respectively. The distribution function is given in terms of g_j or N_j $(= g_j/|\alpha_j|^2)$. The particle polarizability may be written as $|\alpha_0|M_j$, as noted at Eq. 7.1, where M_j is the mass of the particle belonging to the j-th group. We must note that Γ defined in Eq. 7.2 is a complicated function of τ, unless the solution is monodisperse.

If Γ_j is a continuous variable, we can write Eq. 7.2 as

$$g^{(1)}(\tau) = \int_0^\infty G(\Gamma)\mathrm{e}^{-\Gamma\tau}\mathrm{d}\Gamma = \int_0^\infty G(x)\mathrm{e}^{-x\tau}\mathrm{d}x \tag{7.3}$$

where $G(\Gamma)$ is the normalized characteristic linewidth distribution function. But, in Eq. 7.3, Γ works as an integration variable, x.

If the time correlation function is obtained by observing the fluctuating scattered light intensities, it is the second-order correlation function, $g^{(2)}(\tau)$, from which $g^{(1)}(\tau)$ can be obtained. But, these inherently contain noise. This noise is particularly bothersome for a polydisperse system, since it is not easy to smooth out the noise. If the decay time of the correlation function is too fast, the electronic device may not be fast enough and fails to work well. Then, the first-order correlation function in the ω domain is obtained by a spectrograph. It must have the form:

$$g^{(1)}(\omega) = \frac{1}{\pi\sum g_j}\sum_j \frac{g_j\Gamma_j}{(\omega-\omega_0)^2+\Gamma_j^2} = \frac{1}{\pi}\int_0^\infty G(x)\frac{x}{(\omega-\omega_0)^2+x^2}\mathrm{d}x \tag{7.4}$$

If the frequency resolution is poor, an interferometer may be used.

Equation 7.3 is the Laplace transform of $G(x)$. If the unknown $G(x)$ is to be obtained from the experimentally observed $g^{(1)}$, which may be obtained from

$(g^{(2)}-1)^{1/2}$, the procedure involved is the Laplace-transform inversion. However, the integration limits are finite instead of null and infinity because of the finite range of τ in the measurement of $g^{(1)}$. Thus, the observed correlation function contains noise and is bandwidth-limited. Unless $g^{(1)}$ is clean, any rigorous numerical procedure cannot be successful. If there is any additional information, such as the $G(M)$ (M: particle mass) obtained by the static light scattering, available for use in the analysis, it would be very helpful. If the line shape in the frequency domain can be simultaneously observed (Exercise 7.1), the analysis in the frequency domain may be used. In recent years, much attention has been focussed on the inversion problem associated, in particular, with the finite bandwidth and noise.

The recommended bandwidth to be used is such that $g^{(1)}(\tau_{\min})<0.998$ and $g^{(1)}(\tau_{\max})>0.005$ (Chu, 1991, p. 247). We must be sure that the detector area is smaller than the coherent area (Eq. 6.15). Previously, we considered that scattered light only comes from particles, but a correction is needed if the solvent is also involved in the scattering (Chu, 1991, p. 296). Provencher (1982) has introduced a program, known as COIN, to smooth the observed $g^{(1)}$. Comparable to this is the method of maximum entropy (Livesey et al., 1986; Vansco et al., 1988; Nyeo and Chu, 1989; Bryan, 1990). Before using the above methods in the inversion, it is usually desirable to have some preliminary idea about the shape of $G(\Gamma)$. There are a few approximate methods.

A. Double-exponential method. By adjusting a few parameters, g_1, Γ_1 and Γ_2, in the form

$$g^{(1)}(\tau) = g_1 \exp(-\Gamma_1 \tau) + g_2 \exp(-\Gamma_2 \tau) \tag{7.5}$$

with $g_1+g_2=1$, Eq. 7.5 is made to best fit the observed $g^{(1)}(\tau)$ over the experimental range of τ by means of a non-linear least square method (Bevington, 1969). Equation 7.5 defines the theoretical $g^{(1)}_{\text{th}}(\tau)$. Experimentally, $g^{(1)}_{\text{exp}}(\tau)$ is measured at τ_i for i from 1 to N. Then the quantity, χ^2 (Chi squared), is defined by

$$\chi^2(g_1, \Gamma_1, \Gamma_2) = \sum_1^N \frac{[g^{(1)}_{\text{th}}(\tau_i) - g^{(1)}_{\text{exp}}(\tau_i)]^2}{g^{(1)}_{\text{exp}}(\tau_i)} \tag{7.6}$$

Now, choose the values of the parameters so that the χ^2 is minimum ($d\chi^2/dg_1=0$, etc.).

Finally, the result is expressed as

$$G(\Gamma) = g_1 \delta(\Gamma - \Gamma_1) + g_2 \delta(\Gamma - \Gamma_2) \tag{7.7}$$

corresponding to a two-size system. This gives an average, $\langle\Gamma\rangle = g_1\Gamma_1+g_2\Gamma_2$, and the variance, $g_1(\Gamma_1-\langle\Gamma\rangle)^2+g_2(\Gamma_2-\langle\Gamma\rangle)^2$, of the size distribution function. Although the assumption is crude, Eq. 7.5 must fit the observed $g^{(1)}$ for a broad range of τ, but the application is limited (King and Treadaway, 1977).

B. Cumulant method. This has been most commonly practiced in analysis. The logarithm of the experimentally observed correlation function is fitted to a power series expansion in $(-\tau)$ in the form

$$\begin{aligned}\ln g^{(1)}(\tau) &= (1/2)\ln(g^{(2)} - 1)\ , \\ &= C_0 - K_1\tau + (1/2!)K_2\tau^2 - (1/3!)K^3\tau^3 + \cdots\end{aligned}$$

so that the expansion coefficients, K_1, K_2,$\cdots$, are found, where K_1, K_2, K_3,$\cdots$ are known as the cumulants, in statistics. C_0 is expected to be unity but depends on the choice of the experimental baseline which is affected by the noise. The cumulants are interpreted in terms of the average diffusion constant as follows.

The logarithm of Eq. 7.2 can be easily expanded into Taylor's series with coefficients (Exercise 7.2)

$$K_n = (-1)^n \frac{\mathrm{d}^n}{\mathrm{d}\tau^n} \ln g^{(1)}(\tau)|_{\tau=0} \tag{7.9}$$

Thus, the explicit forms of the first few cumulants are

$$\begin{aligned}K_1 &= \langle \Gamma \rangle = \sum g_j \Gamma_j / \sum g_j \\ K_2 &= \langle (\Gamma - \langle \Gamma \rangle)^2 \rangle = \sum g_j (\Gamma_j - \langle \Gamma \rangle)^2 / \sum g_j \\ K^3 &= \langle (\Gamma - \langle \Gamma \rangle)^3 \rangle \\ K^4 &= \langle (\Gamma - \langle \Gamma \rangle)^4 \rangle - 3K_2^2\end{aligned} \tag{7.10}$$

Usually, the experimental accuracy of the higher moments is poor, so that this analysis may be most effective for a unimodal distribution. The assumptions here are as follows: (a) no interactions between scatterers (sufficiently dilute) and (b) no interparticle interference (small scatterers or small q). K_1 indicates the average and K_2 the variance of the distribution. K_3 and K_4 are the skewness (asymmetry) and the kurtosis (peakedness or flatness), respectively. If K_3 and K_4 vanish, the distribution is Gaussian. Therefore, the data are good for small τ and the analysis may be simple, only if K_1 and K_2 are involved. If K_2/K_1^2 is less than 0.02, the disperse system may be considered monodisperse. This method of analysis has been experimentally demonstrated with polystyrene latex spheres (Bargeron, 1974). If K_1 and K_2 are obtained as a function of scattering directions, additional information about the size distribution may be obtained. Of course, the characteristic linewidth may be a complicated function of the scattering vector.

Note that the variance of $G(\Gamma)$ is given by the expansion coefficient, K_2. If $K_2/\langle \Gamma \rangle^2 < 0.3$, the mean, $\langle \Gamma \rangle$, and the variance can be fairly reliably obtained without prior knowledge and can be used for a further detailed analysis.

C. Histogram method. This method may be used for multimodal distributions. The particle sizes (or weights) in the range of the observed size, Γ, are divided into a small number of groups, so that the distribution function is expressed by the magnitude, g_i, of each group i (histogram). The g_i may be interpreted as a relative number of the particles belonging to the i-th group, for which the value of Γ is Γ_i. Then the correlation function, $g^{(1)}(\tau)$, can be calculated by Eq. 7.2 if we know g_i for all i.

As for the distribution function, g_i's are treated as adjustable parameters. The values are so chosen that the calculated correlation function agrees best with the experimental correlation function over the wide range of τ. This method offers a fairly accurate determination of $G(\Gamma)$ without independent knowledge of the form of the distribution function (see Gulari et al., 1979).

If the distribution function is determined for a given polydisperse system, the degree of the polydispersity may be defined by the standard deviation:

$$\sigma_\Gamma = \langle (\Gamma - \langle \Gamma \rangle)^2 \rangle \tag{7.11}$$

This is simply a measure of the spread of the distribution.

7.2 Monodisperse Systems

If polydisperse systems contain rather large nonspherical particles, the meaningful size distribution function is almost impossible to be experimentally determined. In particular, if particles belonging to different size groups interact with each other, the interpretation of the distribution function, as defined by Eq. 7.3, is difficult. In addition, there are countless important applications of monodisperse systems in ceramics, catalysis, pigments, recording materials, medical diagnostics, etc. (Candau and Ottewill, 1990). Their great significance to basic research has also been recognized. One historic example is Perrin's famous work (1909) on Avogadro's number with monodisperse spheres of gamboge, obtained by patiently repeated fractional centrifugation.

There are abundant literature dealing with the synthesis and characterization (Pieranski, 1983; Y. Kawashima et al., 1991; Meakin and Skjeltorp, 1993; Matijević, 1994) of monodispersed microspheres.

Significant progress has been made in preparation of monodisperse systems of various materials by precipitation and swollen emulsion polymerization. However, chemical and physical mechanisms of the formation and growth are not well known because of the complexity of processes involved. There are two essential aspects of the formation; the chemical processes leading to their precipitation and the mechanism of particle nucleation and growth.

In the same way as discussed in Chapt. 3, homogeneous nucleation will occur when solutions are supersaturated with solute concentrations by sudden changes

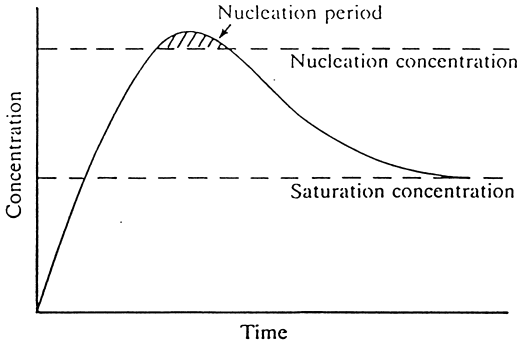

Fig. 7.1 Solute concentration change in time (Overbeek, 1981, with permission from Royal Australian Chemical Institute).

in temperature, pressure, or mixing of two soluble materials that react to form an insoluble species. But, even at the supersaturated state, the first crystal nuclei are sometimes hard to form since it has a large surface curvature and so requires a large free energy. Once a few nuclei are formed, however, precipitation proceeds rapidly since energy is released both by the precipitation from the surrounding supersaturated solution and by the reduction of the surface curvature as the crystal grows. If a roughened foreign surface or a seed is introduced, precipitation follows at once (heterogeneous precipitation).

From solutions just beyond saturation, it takes time for any nucleation to occur and a few large crystals are formed. From highly saturated solutions many small crystals are formed. After the first burst of nucleation, subsequent precipitation occurs on the already formed nuclei. Therefore, in order to create monodisperse systems, the conditions must be created so that nucleation occurs in a single short burst. The nuclei grow by precipitation rapidly at first and the solute concentration falls below the precipitation (Fig. 7.1) so that the particle number remains constant and all grow together to the same size.

The initial particle size distributes with a certain spread. If the subsequent precipitation rate is proportional to the particle surface area, the final size distribution in volume then becomes narrower. If the incorporation of material into the particle occurs by particle aggregation or emulsion polymerization at the same rate for all particle sizes, the size distribution narrows more markedly. In these processes, polydispersity commonly decreases in time. A reversing process is Ostwald's ripening, which has an effect for larger particles to grow at the expense of smaller particles, as discussed later at Eq. 7.12. This reversing tendency, however, is insignificant, provided the particle solubility is very low so that there is not enough time to establish equilibrium. Therefore, precipitation, polymerization, or aggregation is very effective in producing monodisperse systems from highly insoluble materials, such as metal (hydrous) oxides, halides, sulfides, selenites, phosphates, carbonates, etc.

The aggregation mechanism of monodisperse formation has been established in many cases, as discussed below, but qualitatively not well known. A more difficult problem is probably the morphology of the precipitated solid (Matijević, 1994). In some cases, the shape is related to the chemical compositions, but, in

many cases, it appears in different geometries even though the experimental conditions are nearly the same.

In 1857 Faraday reported light scattering from gold sols. Zsigmondy developed the seed method for consistently producing stable monodisperse gold sols. He showed that the small differences in size among the initial seeds ($\sim$3 nm) were rapidly smoothed out as the crystals grew. La Mer and Dinegar (1950) prepared monodisperse sulfur sols from acidified thiosulfate solutions. They allowed a large number of nuclei to form in the first preparation and then to grow by adding of more reactants just below the supersaturation level. Watillon and Dauchot (1968) produced monodisperse selenium sols of 4–50 nm by precipitation of selenium on to gold nuclei for better size control by eliminating homogeneous precipitation. Synthetic methods to obtain sols of metal oxides from precipitation are discussed by Matijević (1985). Ottewill and Woodbridge (1961) obtained monodisperse silver iodide and silver bromide sols by diluting a solution of a complex silver halide ion to form supersaturated solutions of the silver halide. Particle size was about 400 nm.

Monomers, such as styrene, may be made soluble in water by surfactants. The emulsified monomers will react with a water-soluble initiator, say H_2O_2, to form a free radical, which may be water insoluble. On the other hand, a sufficient amount of a surfactant present in the solution forms a large number of surfactant aggregates, called micelles (see Sec. 2.3; Chapt. 9). The resulting free radical is solubilized in these micelles, where it quickly reacts with solubilized monomer to form polymer. The polymer chains grow in micelles until the process is terminated by reaction with another radical. The resulting dispersion is called latex. This emulsion polymerization technique (El-Aasser, 1990) is well suited to the production of small (1 μm or less) particles. Larger particles are formed by the addition of more monomers to the suspension, but this process yields rather broad size distribution. However, the swollen emulsion polymerization technique (Ugelstad et al., 1983), achieved by adding a swelling agent such as dodecyl chloride, allows the production of very uniform spheres with diameters ranging from 1 to 100 μm and a standard deviation in diameter of less than 1%. The swelling agent causes the particles to swell by imbibing a large amount of monomers. These monodisperse microspheres used in the separation column as a packing have led to a dramatic increase in speed and resolution achieved by liquid chromatography.

In emulsion polymerization, polymer growth occurs slowly after the initiation of polymerization, the narrow distribution of micellar sizes narrows even further as the particle grows. The optimum conditions for the formation of monodisperse suspensions are determined empirically.

Ugelstad et al. (1988) produced magnetizable spheres of size 5 to 10 nm by deposition of magnetic iron oxide in the porous texture of the particles (see also Bate, 1991). The particles have almost no hysteresis in the magnetization curve (Berge et al., 1990). The swollen emulsion polymerization technique can also be used to produce nonspherical particles (Vanderhoff et al., 1990).

Monodisperse systems have been hardly formed in solutions under the presence of condensed electrolytes since an aggregation easily occurs. An exception to this is the formation of monodisperse silver-halide particles in a gelatin environment.

If the solution is transformed to a gel state, Brownian motion of the grown particles is suppressed from aggregation, thus a monodisperse system of hematite particles could have been produced (Shindo et al., 1993).

Because of the complexity of the mechanism involved in the monodisperse formation, the production is very often of empirical nature without a theoretical understanding. In Chapt. 3, we treated nucleation in a two-phase system up to the formation of stable critical particles. But here, we are concerned with a formation of a uniform disperse system in a well-stirred open system with a constant feed of the monomer source. Sugimoto (1992) treated this system by assuming that the monomer source instantly reacts to form embryos with a definite size distribution function. The dissolution and growth of the embryos are limited by diffusion of monomers due to the Ostwald effect.

The Ostwald effect occurs as follows. Suppose that there are two embryos of radii r_1, and r_2, which are locally in equilibrium with monomers in the solution. We denote by c_1 the number density of monomers in equilibrium with the embryo of radius r_1. This c_1 is proportional to the saturated partial pressure, p', of monomers at the surface of the embryo. Using the Kelvin equation (Exercises 2.4 or 3.2) we have

$$\ln(c_1/c_\infty) = 2\gamma v_\mathrm{m}/(r_1 k_\mathrm{B} T) \tag{7.12}$$

where c_∞ is the number density of monomers in equilibrium with the bulk solid (hypothetically, an embryo of a large radius) and v_m is the volume of a monomer in the solid (embryo) phase. Thus,

$$v_\mathrm{m} = V_\mathrm{m}/N_\mathrm{A} \tag{7.13}$$

where V_m is the molar volume of monomers in the embryo phase, as defined in Exercise 3.2 and N_A is the Avogadro number. Similarly, for the embryo of radius, r_2, we have

$$\ln(c_2/c_\infty) = 2\gamma v_\mathrm{m}/(r_2 k_\mathrm{B} T) \tag{7.14}$$

If $c_2 > c_1$ ($r_2 < \mathrm{r}_1$), we can expect a diffusion of monomers from the embryo of the smaller radius to that of the larger radius and the larger embryo can grow at the expense of the smaller embryo. However, unless the size of embryos is small (10 nm or less), this effect is small.

Suppose that a constant monomer source is present in the solution and generates embryos far apart from each other (at distances more than 10 times the diameter of a typical embryo). Consider a spherical embryo of radius r surrounded by monomers of a number density c_r at the surface and of c in the bulk. Assuming the spherical symmetry around the embryo and using a radial coordinate ρ, the diffusion equation can be written as

$$\frac{\partial c(\rho,t)}{\partial t} = D\left[\frac{\partial^2 c(\rho,t)}{\partial \rho^2} + \frac{2}{\rho}\,\frac{\partial c(\rho,t)}{\partial \rho}\right] \tag{7.15}$$

where $c(\rho, t)$ is the number density of monomers at ρ and t and D is the diffusion coefficient of the monomers. If the diffusion is fast, the quasi-steady state $(\partial c(\rho, t)/\partial t \sim 0)$ is set up faster than the embryo grows and

$$c(\rho) = c_r + (c - c_r)(1 - r/\rho) \tag{7.16}$$

Here, c_r is the solubility at the embryo of radius, r. Then, the rate of increase of the number of monomers in the embryo of radius, r, is $4\pi r^2 D(\mathrm{d}c/\mathrm{d}\rho)_{\rho=r}$. Since the rate of the volume change is $4\pi r^2(\mathrm{d}r/\mathrm{d}t)$, we have

$$\frac{\mathrm{d}r}{\mathrm{d}t} = D v_\mathrm{m}\left(\frac{\mathrm{d}c}{\mathrm{d}\rho}\right)_{\rho=r} = D v_\mathrm{m}\frac{c - c_r}{r} \tag{7.17}$$

(Nielsen (1961) solved the problem exactly.)

Denote by r^* the radius of the embryo which is in equilibrium with the bulk concentration c, and then we write the similar equation as Eq. 7.14 for (r, c_r) and (r^*, c). Assuming that c/c_∞ and c_r/c_∞ are about unity each, the above equation can be approximately given by

$$\frac{\mathrm{d}r}{\mathrm{d}t} = D\frac{2\gamma v_\mathrm{m}^2 c_\infty}{k_\mathrm{B}T}\cdot\frac{r - r^*}{r^* r^2} \tag{7.18}$$

Note that $\mathrm{d}r/\mathrm{d}t$ depends on r^{-1} for $r \gg r^*$.

There are many other different ways in which the suspended embryos can grow (see Nielsen, 1964). Here, the rate of growth is assumed to be controlled by diffusion, but the result may be applicable to reaction-limited cases if D is replaced by other parameters.

In photographic emulsions, monodisperse AgBr particles are formed by simultaneously introducing two solutions of silver nitrate and potassium bromide to a well-stirred aqueous solution of inert gelatin. The gelatin protects the existing particles against coagulation and secondary nucleation. By the chemical reaction, embryos are assumed to be instantaneously formed with a normalized distribution function, $f_\mathrm{embr}(r)$, of size, r, carrying an upper bound at $r = r_\mathrm{p}$. If the embryos are larger than some critical size r^*, they grow according to Eq. 7.18. If their grown size is larger than r_p, they are called stable particles, but if they are still smaller than r_p, they have chances to dissolve by the Ostwald effect and called unstable particles.

The value of r^* is determined by the bulk concentration of monomers, c. At the beginning of the monomer feed r^* is very large. But as the feed proceeds, r^* decreases and eventually becomes smaller than r_p. Monomers, then, start to be used for particle growth in the solution and r^* increases in size. The nucleation always starts from embryos, which have an upper limit in size, so that when r^* surpasses r_p new nucleation of stable nuclei stops.

In the present open model, monomers are constantly added and the distribution function, $f(r,t)$, of particles satisfies the balance or continuity equation (Reichl, 1980, p. 660):

$$\frac{\partial f}{\partial t} = -\frac{\partial}{\partial r}\left(\frac{\mathrm{d}r}{\mathrm{d}t} f\right) + N_0 f_{\mathrm{embr}}(r) \tag{7.19}$$

where N_0 is the number of the embryos generated, per unit time, immediately when the monomers are added to the system. As we see, therefore, $f(r,t)$ is not normalized. Namely, $f(r,t)\mathrm{d}r$ is the number of particles of size between r and r+dr in the solution.

In Secs. 3.2 and 9.1, we have discussed formation of embryos or the like. We can see, however, that it is impossible to theoretically calculate $f_{\mathrm{embr}}(r)$ with an upper bound r_{p} without introducing a new model.

The number of unstable particles $n_{\mathrm{u}}(t)$ at time t is given by

$$n_{\mathrm{u}}(t) = \int_0^{r_{\mathrm{p}}} f(r,t)\mathrm{d}r \tag{7.20}$$

After r^* has exceeded r_{p}, the number of stable nuclei ceases to increase and the unstable nuclei ($r \leq r_{\mathrm{p}}$) remain in a quasi-steady state of balance between their generation and dissolution. Then, $\partial f/\partial t \simeq 0$ for unstable nuclei and we have from Eqs. 7.18 and 7.19

$$f(r,t) = n_0 \frac{r^* r^2}{r - r^*} \int_{r^*}^{r} f_{\mathrm{embr}}(r)\mathrm{d}r \ , \tag{7.21}$$

where

$$n_0 = N_0 k_{\mathrm{B}} T/(2D\gamma v_{\mathrm{m}}^2 c_\infty) \tag{7.22}$$

The approximation of Eq. 7.21 does not hold for unstable particles. Substituting Eq. 7.21 into Eq. 7.20, we have $n_{\mathrm{u}}(t)$. Since the added monomers are used for both particle growth and the nucleation of new particles, the concentration of monomers in the bulk solution, after having reached maximum, decreases and r^* increases to a very large value. In the limit of $r^* \to \infty$, the number of unstable particles, n_{u}^{∞}, is given by

$$n_{\mathrm{u}}^{\infty} = n_0 \int_0^{r_{\mathrm{p}}} \mathrm{d}r r^2 \int_r^{r_{\mathrm{p}}} \mathrm{d}r' f_{\mathrm{embr}}(r') \tag{7.23}$$

By integration by parts, we find

$$n_u^{\infty} = \frac{n_0}{3}\int_0^{r_p} r^3 f_{embr}(r)\mathrm{d}r = \frac{n_0}{4\pi}v_0 \tag{7.24}$$

where v_0 is the mean volume of embryos. This result does not depend on the detailed shape of the distribution function, except for the presence of the cutoff at r_p. Thus, the number of unstable particles converges to a finite number, $n_0 v_0/4\pi$.

The number of stable particles at time t is given by

$$n_s(t) = \int_{r_p}^{\infty} f(r,t)\mathrm{d}r \tag{7.25}$$

Note that Eq. 7.21 cannot be used for stable particles. These stable particles have been created from embryos larger than r^* and grown through the size r_p. These particles keep growing as long as $r > r^*$. The rate of increase in the number of stable particles, n_s, is given by the flux, $f(r,t)$ ($\mathrm{d}r/\mathrm{d}t$), in the population space at $r = r_p$. Thus,

$$\frac{\mathrm{d}n_s}{\mathrm{d}t} = f(r,t)\frac{\mathrm{d}r}{\mathrm{d}t}\bigg|_{r=r_p} = N_0\int_{r^*}^{r_p} f_{embr}(r)\mathrm{d}r \tag{7.26}$$

Note that r^* increases with time, causing a change in n_s. If $r^* = r_p$, $\mathrm{d}n_s/\mathrm{d}t = 0$ and, after that, n_s becomes constant (n_s^{∞}).

The increment of the total volume of the stable nuclei for a unit of time under the quasi-steady condition of the unstable particle is given by

$$N_0 v_0 = 4\pi\int_{r_p}^{\infty} f r^2 \frac{\mathrm{d}r}{\mathrm{d}t}\mathrm{d}r + v_p\frac{\mathrm{d}n_s}{\mathrm{d}t} \tag{7.27}$$

where $v_p = (4\pi/3)r_p^3$, the volume of the particle at $r = r_p$. The second term on the right hand side is the contribution to the increment due to the flux of particles from the region of unstable particles and the first term is due to the growth rate of the particle volume. By using Eqs. 7.18, 7.25, and 7.26, Eq. 7.27 yields

$$n_s\left(\frac{r_s}{r^*} - 1\right) = \tau N_0\left(\frac{v_0}{v_p} - x^*\right) \tag{7.28}$$

where r_s is the mean radius of the stable particles, given by

$$r_s = \int_{r_p}^{\infty} fr\mathrm{d}r \Big/ \int_{r_p}^{\infty} f\mathrm{d}r$$

and τ and x^* are defined by

$$\tau = \frac{k_B T}{8\pi D\gamma v_m^2 c_\infty} \quad \text{and} \quad x^* = \int_{r^*}^{r_p} f_{embr}(r)\mathrm{d}r \tag{7.29}$$

Now, if we know $f_{embr}(r)$, we can find the minimum value, r^*_{min}, of r^*. For simplicity, we assume that the nucleation starts when r^* reaches its minimum. If we set the origin of time when $r^* = r^*_{min}$, we have $f(r,0)=0$ and $n_s(0)=0$. From Eq. 7.28, at r^*_{min}

$$v_0/v_p = x^* \tag{7.30}$$

Sugimoto (1992) assumed that

$$f_{embr}(r) = (2/r_p)\sin^2(\pi r/r_p) \quad \text{for} \quad 0 < r < r_p \tag{7.31}$$

This function is symmetric about the maximum at $r=r_p/2$ and has the halfwidth of $r_p/2$. Then, $v_0/v_p=0.1740$ and Eq. 7.30 gives

$$r^*_{min}/r_p = 0.6814 \tag{7.32}$$

He also obtained the total number and the mean size of the stable particles when r^* reaches r_p.

$$n_s^\infty = \frac{1.567 N_0 v_0 k_B T}{8\pi D\gamma v_m^2 c_\infty}, \quad \text{and} \quad r_s = 1.638 r_p \tag{7.33}$$

Then, from Eq. 7.28, the ratio of r_s/r^* is maintained after r^* has reached r_p.

$$r_s/r^* = 1.638 \tag{7.34}$$

Sugimoto (1992) showed that his theoretical prediction was in good agreement with his experimental results on the AgBr systems.

Exercises

7.1 Under what condition can $g^{(1)}(\omega)$ be observed in the frequency domain? (Refer to Fig. 6.3.)

7.2 Show that Eq. 7.3 leads to

$$g^{(1)}(\tau) = \int_0^\infty G(\Gamma)\left(1 + \sum_{n=1}^{\infty}(-1)^n \frac{1}{n!}\Gamma^n\tau^n\right)\mathrm{d}\Gamma$$

where $\langle\Gamma\rangle = \int G(\Gamma)\Gamma\mathrm{d}\Gamma$. The correlation function, $g^{(1)}(\tau)$, can thus be written in terms of moments about zero as

$$g^{(1)}(\tau) = 1 + \sum_{n=1}^{\infty}(-1)^n \frac{1}{n!}\nu_n\tau^n\ , \quad \nu_n = \int_0^\infty G(\Gamma)\Gamma^n\mathrm{d}\Gamma$$

Note that $\nu_1 = \langle\Gamma\rangle$. Using this expression and Eq. 7.9 and noting that

$$\frac{\mathrm{d}\ln g^{(1)}(\tau)}{\mathrm{d}\tau} = \frac{1}{g^{(1)}(\tau)}\frac{\mathrm{d}g^{(1)}(\tau)}{\mathrm{d}\tau}$$

verify Eq. 7.10.

7.3 Establish Eq. 7.17

7.4 Using Eq. 7.17, find the dissolution time for a particle with $r(t=0) = 100$ Å when the bulk concentration is zero. Assume that $v_\mathrm{m} = 0.1$ liter/mol, $D = 10^{-5}$ cm^2/s and $c_r = 10^{-10}$ mol/liter.

7.5 Establish Eq. 7.18 by approximating Eqs. 7.12 and 7.14.

7.6 Give a possible way the suspended embryo can grow. (A chemical or physical reaction at the two-dimensional surface can more easily lead to the embryo growth than the formation of new embryos in the three-dimensional solution (Volmer and Weber, 1926). In this mechanism, $\mathrm{d}r/\mathrm{d}t = kv_m(c_r - c_\mathrm{e})$, where c_e is the equilibrium monomer concentration. The surface concentration c_r is held by diffusion (Eq. 7.17). If we eliminate c_r between this equation and Eq. 7.17, we have a relation for the presence of both the reaction at the surface and the diffusion.)

7.7 Show that Eq. 7.28 is equal to

$$\frac{4\pi}{3}\int_{r_\mathrm{p}}^\infty \frac{\partial f}{\partial t}r^3\mathrm{d}r$$

for the stable particles.

7.8 Verify Eq. 7.32.

References

Bargeron, C.B., *J. Chem. Phys. 61*, 2134 (1974).

Bate, G., *J. Magn. Mater. 100*, 413 (1991).

Berge, A., Ellingsen, T., Skjeltorp, A., and Ugelstad, J., "Scientific Methods for the Study of Polymer Colloids and their Applications", eds. Candau, F. and Ottewill, R.H., Kluwer, Dordrecht (1990), p. 435.

Bevington, P.R., "Data Reduction and Error Analysis for the Physical Sciences", McGraw-Hill, New York (1969).

Bryan, B.K., *Eur. Biophysics J. 18*, 165 (1990).

Candau, F. and Ottewill, R.H., eds., "Scientific Methods for the Study of Polymer Colloids and their Applications", Kluwer, Dordrecht (1990).

Chu, B., "Laser Light Scattering", 2nd ed., Academic Press Inc., New York (1991).

El-Aasser, M.S., in "Scientific Methods for the Study of Polymer Colloids and their Applications", eds. Candau, F. and Ottewill, R.H., Kluwer, Dordrecht (1990), p. 1.

Ford, N.C.,Jr., Gabler, R. and Karasz, F.E., *Adv. Chem. 125*, 25 (1873).

Gulari, E., Tsunashima, T., and Chu, B., *J. Chem. Phys. 70*, 3965 (1979).

Kawashima, Y., Hino, T., Takeuchi, H., Niwa, T., and Horibe, K., *J. Colloid Interface Sci.*, *145*, 512 (1991).

King, T.A. and Treadaway, M.F., *J. Chem. Soc. Faraday Trans. II 73*, 1616 (1977).

La Mer, V.K. and Dinegar, R.H., *J. Am. Chem. Soc. 72*, 4847 (1950).

Livesey, A.K., Licinio, P., and Delaye, M., *J. Chem. Phys. 84*, 5102 (1986).

Matijević, E., *Annu. Rev. Mater. Sci. 15*, 483 (1985).

Matijević, E., *Langmuir 10*, 8 (1994).

Meakin, P. and Skjeltorp, A., *Adv. Phys. 42*, 1 (1993).

Nielsen, A.E., *J. Phys. Chem. 65*, 46 (1961).

Nielsen, A.E., "Kinetics of Precipitation", Pergamon, Oxford (1964).

Nyeo, S.-L. and Chu, B., *Macromolecules 22*, 3998 (1989).

Ottewill, R.H. and Woodbridge, R.F., *J. Colloid Sci. 16*, 581 (1961).

Overbeek, J.Th.G., *Chem. Austral. 48*, 419 (1981).

Pieranski, P., *Contemp. phys. 24*, 25 (1983).

Provencher, S.W., "CONTIN Users Manual", EBL Technical Report DA05, European Molecular Laboratory, Heidelberg (1982).

Reichl, L.E., "A Modern Course in Statistical Physics", University of Texas Press, Austin (1980).

Schnablegger, H. and Glatter, O., *J. Colloid Interface Sci. 158*, 228 (1993).

Shindo, D., Aito, S., Park, P., and Sugimoto, T., *Materials Transactions, JIM34*, 1226 (1993).

Sugimoto, T., *J. Colloid Interface Sci. 150*, 208 (1992).

Ugelstad, J., Stöderberg, L., Berge, A., and Bergström, J., *Nature 303*, 95 (1983).

Ugelstad, J., Mfutakamba, H.R., Mork, P.C., Ellingsen, T., Berge, A., Schmid, R., Holm, L., Jorgedal, A., Hansen, F.K., and Nustad, K., *J. Polym. Sci. Polym. Symp. 72*, 225 (1985).

Ugelstad J., Berge, A., Ellingsen, T., Aune, O., Kilaas, L., Nilsen, T.N., Schmid, R., Stenstad, P., Funderud, S., Kvalheim, G., Nustad, K., Lea, T., Vartdal, F., and Danielsen, H., *Makromol. Chem. Makromol. Symp. 17*, 117 (1988).

Vanderhoff, J.W., Sheu, H.R., and El-Aasser, M.S., "Scientific Methods for the Study of Polymer Colloids and their Applications", eds. Candau, F. and Ottewill, R.H., Kluwer, Dordrecht (1990), p. 529.

Vansco, G., Tomka, I., and Vansco-Polacsek, K., *Macromolecules 21*, 415 (1988).

Volmer, M. and Weber, A., *Z. Phys. Chem. 119*, 277 (1926).

Watillon, A. and Dauchot, J., *J. Colloid Interface Sci. 27*, 507 (1968).